Chemistry
A European
Journal

Chemistry Europe
European Chemical Societies Publishing

Accepted Article

Title: Hybridorubrins A–D, novel azaphilone heterodimers from stromata of Hypoxylon fragiforme and insights into the biosynthetic machinery for azaphilone diversification

Authors: Kevin Becker, Sebastian Pfütze, Eric Kuhnert, Russell Cox, Marc Stadler, and Frank Surup

To be cited as: *Chem. Eur. J.* 10.1002/chem.202003215

Link to VoR: https://doi.org/10.1002/chem.202003215

WILEY-VCH

10.1002/chem.202003215

WILEY-VCH

FULL PAPER

Hybridorubrins A−D, novel azaphilone heterodimers from stromata of *Hypoxylon fragiforme* and insights into the biosynthetic machinery for azaphilone diversification

Kevin Becker,[a] Sebastian Pfütze,[a] Eric Kuhnert,[b] Russell J. Cox,[b] Marc Stadler,*[a] Frank Surup*[a]

Abstract

The diversity of azaphilones in stromatal extracts of the fungus *Hypoxylon fragiforme* was investigated and linked to their biosynthetic machineries using bioinformatics. Nineteen azaphilone-type compounds were isolated and characterized by NMR spectroscopy and mass spectrometry, with their absolute stereoconfigurations assigned using Mosher ester analysis and ECD spectroscopy. Four unprecedented bisazaphilones, named hybridorubrins A−D (**1**−**4**), were elucidated, in addition to new fragirubrins F−G (**5**−**6**) and various known mitorubrin derivatives. Only the hybridorubrins, which are composed of mitorubrin and fragirubrin moieties, exhibited strong inhibition of *Staphylococcus aureus* biofilm formation. Analysis of the genome of *H. fragiforme* revealed the presence of two separate biosynthetic gene clusters (BGC) *hfaza1* and *hfaza2* responsible for azaphilone formation. While the *hfaza1* BGC likely encodes the assembly of the backbone and addition of fatty acid moieties to yield the (*R*)-configured series of fragirubrins, the *hfaza2* BGC contains the necessary genes to synthesise the widely distributed (*S*)-mitorubrins. This study is the first example of two distant cross-acting fungal BGC collaborating to produce two families of azaphilones and bisazaphilones derived thereof.

Introduction

The Hypoxylaceae, which were recently resurrected in the course of a major phylogenetic study, are the second largest family of the ascomycete order Xylariales,[1] and they are known for a particularly diverse secondary metabolism.[2] In contrast to other families of the order, both their mycelial cultures and their stromata (a mass of fungal tissue that has spore-bearing structures such as ascomata embedded) have been shown to contain diverse pigments and other secondary metabolites. The first of these pigments were reported in 1974 by the Steglich group from *Hypoxylon fragiforme*, the type species of the largest genus of the Hypoxylaceae, and shown to belong to the mitorubrin-azaphilone class of metabolites.[3] Several years later, the same species was subjected to an intensive study and various cytochalasans and other unknown molecules were detected and isolated from the young, growing stromata.[4] In the same study, it was found that the composition of secondary metabolite profiles differs drastically during the vegetative growth period, pointing toward differential activation of secondary metabolite biosynthesis genes. From cultures of the fungus, several different metabolites such as dihydroisocoumarins,[5] a dibenzoxanthenone,[6] various cytochalasans,[7] and small polyketides have been reported.[8] Some of these metabolites were found to possess prominent activities in biological systems, while others, like the complex azaphilones that were recently detected in fossil stromata of *H. fragiforme* and isolated from freshly collected material, constitute unprecedented molecules.[1b]

We have recently started to further evaluate the diversity of secondary metabolites in twelve selected species of the Hypoxylaceae for which we generated high quality genome sequences with the aim of establishing correlations between the biological and chemical diversity in these organisms at the genomic level.[9] The ex-epitype strain of *H. fragiforme*, the type species of the genus *Hypoxylon* and the most frequently encountered species in the Northern hemisphere, was selected for genome sequencing. As expected from the various reports on the chemical diversity of secondary metabolites, the genome harbours a great many biosynthetic gene clusters (BGC) that putatively encode the biosynthesis of various polyketide and polyketide-peptide hybrids. We have recently reported on the identity of the cytochalasin gene cluster of this fungus and its partial heterologous expression in *Magnaporthe grisea* [10]. Furthermore, we reported the occurrence of the novel azaphilones, fragirubrins A−E, as well as the bisazaphilones rutilins C−D, in stromata of *H. fragiforme* in addition to the known mitorubrins.[1b] The present study deals with the isolation and identification of azaphilone heterodimers with interesting structural and biological features as well as the assignment of their biosynthesis genes.

[a] K. Becker, S. Pfütze, Prof. Dr. M. Stadler, Dr. F. Surup
Department Microbial Drugs
Helmholtz Centre for Infection Research GmbH (HZI)
Inhoffenstraße 7, 38124 Braunschweig (Germany)
E-Mail M. Stadler: marc.stadler@helmholtz-hzi.de
E-Mail F. Surup: frank.surup@helmholtz-hzi.de
and
German Centre for Infection Research Association (DZIF)
Partner site Hannover-Braunschweig
Inhoffenstraße 7, 38124 Braunschweig (Germany)

[b] Dr. E. Kuhnert, Prof. Dr. R. J. Cox
Institute for Organic Chemistry, Leibniz University Hannover
Schneiderberg 1B, 30167 Hannover (Germany), and
Centre for Biomolecular Drug Research (BMWZ)
Schneiderberg 38, 30167 Hannover (Germany)

Supporting information for this article is given via a link at the end of the document.

Results and Discussion

Isolation and structure elucidation

Freshly collected stromata of *Hypoxylon fragiforme* were extracted with acetone. In the crude extract the new compounds **1**−**6** (Figure 1) were detected by HR-ESI-MS analysis and subsequently purified by preparative chromatography.

Hybridorubrin A **1** was shown to possess the molecular formula $C_{52}H_{62}O_{15}$ by HR-ESI-MS. The IR spectrum of **1** showed characteristic absorptions at ν_{max} = 1717 and 1621 cm^{-1}, representing ester and conjugated double bonds, respectively (Figure S42). In the ^{1}H and ^{1}H/^{13}C HSQC NMR spectra, the presence of six methyls, two methylenes plus an uncertain number of methylenes in an alkyl chain, as well as nine aromatic/olefinic methines were observed. The ^{13}C and ^{1}H/^{13}C HMBC spectra showed the presence of four conjugated ketones, three carboxylic esters, as well as eleven sp^2- and two sp^3-hybridized carbons.

^{1}H/^{1}H COSY signals (Figure 2) revealed 12-H$_2$, 13-H, and 14-H$_3$ to be contiguous. For the propyl chain 12-H$_a$, 13-H$_a$, and 14-H$_a$, a similar link was established. The first azaphilone core was identified by ^{1}H/^{13}C HMBC correlations (Figure 2) from 3-H to C-2, C-5, and C-10, from 1-H$_2$ to C-3, C-4, C-9, and C-10, as well as from 11-H$_3$ to C-7, C-8, and C-10. Mutual correlations of 5-H and 12-H$_2$ linked C-12 to C-4. An acetate moiety was connected to C-13 by correlations from 13-H to C-15 and from 16-H$_3$ to C-12. The second azaphilone unit was established analogously. Correlations from 13a-H to C-6 as well as 14a-H to C-5, C-6, and C-7 linked both azaphilone units. The (*Z*)-configuration of the $\Delta^{6,14a}$ alkene was deduced from the presence of a strong ^{1}H/^{1}H ROESY correlation between 14a-H and 4-H (*cf.* Figure 2 and S10), while the $\Delta^{12a,13a}$ alkene was determined as (*E*) from the coupling constant of the respective protons (^3J = 15.3 Hz).

For the fatty acid moiety, the carboxylic terminus was established by ^{1}H/^{1}H COSY correlations linking 2'-H$_2$, 3'-H$_2$, and 4'-H$_2$ as well as by ^{1}H/^{13}C HMBC correlations from 3'-H$_2$ to C-1', C-2', C-4', and C-5'. The methyl terminus 16'-H$_3$ showed correlations to C-15' and C-14', which was supported by ^{1}H/^{1}H COSY data. The hydroxy group 13'-OH showed ^{1}H/^{13}C HMBC correlations to C-12', C-13', and C-14'. 12'-H$_2$ had a correlation to C-11', which was accordingly placed in the alkyl chain. The missing carbons C-5' to C-10' were overlapping and could not be assigned unambiguously. Consequently, the length of the fatty acid chain was deduced from the molecular formula of **1**. Using Mosher's method,[11] the stereochemistry of C-13' was assigned as (*R)* (Figure S38), which was found to be identical to lenormandin F.[12] Ultimately, the fatty acid moiety of **1** was deduced to be (*R*)-13'-hydroxypalmitic acid. The fatty acid was linked to C-8 by ^4J-^{1}H/^{13}C HMBC correlations from 11-H$_3$ to C'-1 and from 2'-H$_2$ to C-8. Lastly, the orsellinic acid moiety was established by ^{1}H/^{13}C HMBC correlations of 7a'-H$_3$ to C-1a', C-5a', C-6a', and C-8a', from 4a'-OH to C-3a', C-4a', and C-5a', as well as 2a'-OH to C-1a', C-2a', and C-3a'. Correlations from 11a-H$_3$ to C-8a' linked the orsellinic acid to C-8a'. The stereochemistry of C-8(*R*) and C-8a(*S*) was deduced from their respective building blocks mitorubrin and fragirubrin (see Stereochemistry section below for details).

Analysis of hybridorubrin B **2** revealed its molecular formula to be $C_{54}H_{62}O_{15}$, indicating two additional carbon atoms and two additional degrees of unsaturation compared to **1**. Instead of (*R*)-13'-hydroxypalmitic acid, it bears (*R*)-16'-hydroxylinoleic acid, as shown by its NMR data. The stereochemistry of C-16' was assigned by Mosher's method (Figure S39). The carbon shifts of C-8' and C-14' were characteristic for a *cis (Z)*/*cis* (*Z*) 1,4-diene configuration of $\Delta^{9',10'}$ and $\Delta^{12',13'}$.[13]

Hybridorubrin C **3** had a molecular formula of $C_{54}H_{64}O_{15}$ as shown by HR-ESI-MS data. This implied a formal loss of hydrogen compared to **1**, representing one additional degree of unsaturation. Accordingly, two olefinic protons were observed in in the ^{1}H/^{13}C HSQC spectrum and placed in the fatty acid chain of **3**. The exact position of the alkene was deduced to be $\Delta^{9',10'}$ due to occurrence of two diagnostic MS/MS fragments *m/z* 155.1123 and 171.1066 after epoxidation of the double bond (*cf.* Experimental Section and Figure S45).[14] The stereochemistry of this alkene was determined as *cis* (*Z*) from comparison of chemical shifts of the allylic carbons C-8' and C-11' (both δ_C = 27.4).[15] By applying Mosher's method, the stereochemistry of C-17'(*R*) was deduced (Figure S40).

Hybridorubrin D **4** revealed a molecular formula of $C_{50}H_{60}O_{13}$, implying the formal loss of a $C_2H_2O_2$ fragment compared to **1**. NMR spectra of **4** were highly similar to those of **1**, with the key differences being the lack of an acetyl group attached to O-13 as well as a different fatty acid moiety, which was identified as palmitic acid.

The molecular formula of fragirubrin F **5** was determined by its HR-ESI-MS data as $C_{31}H_{46}O_8$. Its ^{1}H and ^{13}C NMR data showed a high similarity to fragirubrin A **15**.[1b] Compound **5** contains four methyl groups, five olefinic and one aliphatic methines as well as 14 methylenes. Additionally, two conjugated ketones, two ester carbonyls, one oxygenated sp^3-carbon, and three sp^2-carbons were observed in the ^{13}C NMR spectra. The main difference compared to **15** was the replacement of the palmitoyl moiety by (*R*)-14'-hydroxypalmitic acid. The absolute stereochemistry of C-14' was determined using Mosher's method (Figure S41).

HR-ESI-MS data determined the molecular formula of fragirubrin G **6** as $C_{31}H_{44}O_7$, implying one additional degree of unsaturation compared to fragirubrin A **15**. ^{1}H and ^{1}H/^{13}C HSQC spectra located an additional olefin in the fatty acid moiety (C-9'/C-10'). The position and stereochemistry of the double bond was determined by degradation of the sample to its fatty acid methyl ester (**6**-FAME) and subsequent comparison of retention times *via* GC with authentic standards, resulting in the identification of 9-*cis* (*Z*)-hexadecenoic acid (palmitoleic acid; see Figure S46 and Experimental Section).

10.1002/chem.202003215

FULL PAPER

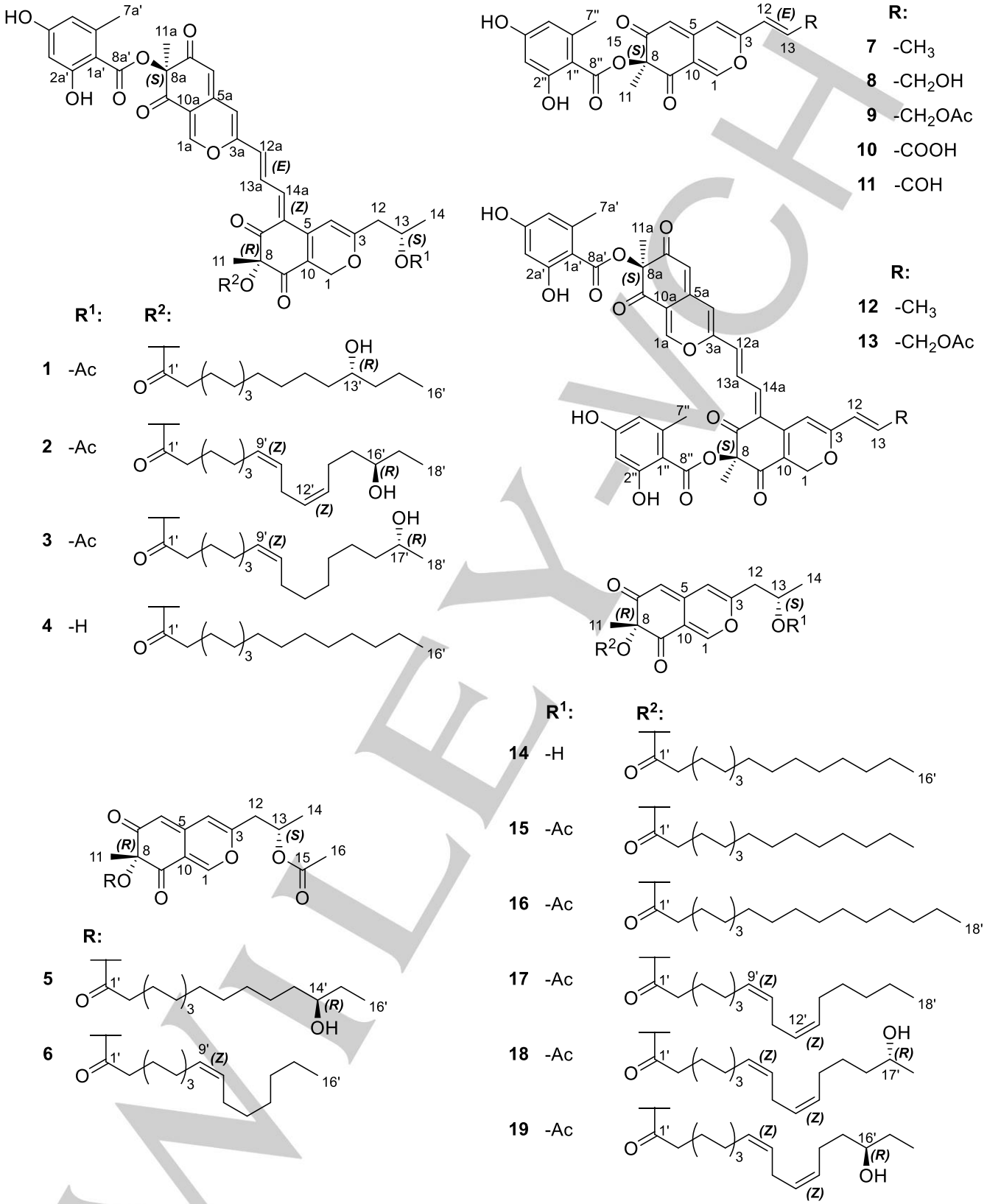

Figure 1. Structures of novel (left) and known (right) azaphilones isolated from the stromata of *Hypoxylon fragiforme*: **1**–**4**: hybridorubrin A–D; **5**–**6:** fragirubrin F–G; **7**: mitorubrin; **8**: mitorubrinol; **9**: mitorubrinol acetate; **10**: mitorubrinic acid; **11**: mitorubrinal; **12**–**13**: rutilin C–D; **14**: lenormandin F; **15**–**19**: fragirubrin A–E.

10.1002/chem.202003215

Table 1. ^{1}H NMR spectroscopic data of hybridorubrins A−D (**1**−**4**) and fragirubrins F−G (**5**−**6**) [**1**, **3**−**4**, **6**: 700 MHz; **2**, **5**: 500 MHz]. Chemical shifts are expressed in ppm.

Position	**1** [a]	**2** [b]	**3** [a]	**4** [a]	**5** [a]	**6** [b]
1	5.07, d (13.6) 4.84, d (13.6)	5.18, d (14.0) 4.87, d (14.0)	5.07, d (13.6) 4.84, d (13.6)	5.02, d (13.6) 4.94, d (13.6)	8.00, d (1.1)	7.85, s
4	6.13, s	5.71, s	6.13, s	6.09, s	6.45, s	6.14, s
6	-	-	-	-	5.47, d (1.1)	5.54, s
11	1.53, s	1.57, s	1.53, s	1.53, m	1.45, s	1.54, s
12	2.63, dd (14.4, 7.7) 2.57, dd (14.4, 5.2)	2.61, dd (14.6, 8.0) 2.49, dd (14.6, 5.0)	2.61, dd (14.3, 8.0) 2.57, dd (14.3, 5.4)	2.46, dd (14.2, 7.7) 2.41, dd (14.2, 5.2)	2.76, d (6.4)	2.69, dd (14.7, 7.3) 2.61, dd (14.7, 5.3)
13	5.19, dqd (7.7, 6.5, 5.2)	5.25, m	5.19, m	4.10, m	5.17, tq (2×6.4)	5.17, m
14	1.30, d (6.5)	1.34, d (6.2)	1.30, d (6.2)	1.22, d (6.2)	1.31, d (6.3)	1.33, d (6.5)
16	1.99, s	2.07, s	1.99, s	-	1.98, s	2.06, s
2’	2.41, t (7.3)	2.46, t (7.7)	2.42, t (7.4)	2.41, t (7.5)	2.36, t (7.4)	2.45, t (7.4)
3’	1.62, m	1.66, m	1.62, td (7.4, 1.8)	1.61, m	1.59, tt (2×7.4)	1.63, m
4’	1.39, m	1.36, m	1.40, m	1.40, m	1.37, m	1.35, m
5’−7’	1.31, m [c]	1.32, m [c]	1.35, m [c]	1.29, m [c]	1.30, m [c]	1.30, m [c]
8’	1.31, m [c]	2.05, m	2.05, m [c]	1.29, m [c]	1.30, m [c]	2.01, m [c]
9’	1.31, m [c]	5.39, m	5.35, m [c]	1.29, m [c]	1.30, m [c]	5.35, m [c]
10’	1.31, m [c]	5.34, m	5.35, m [c]	1.29, m [c]	1.30, m [c]	5.35, m [c]
11’	1.45/1.32, m	2.80, dd (2×6.7)	2.05, m [c]	1.29, m [c]	1.30, m [c]	2.01, m [c]
12’	1.39, m	5.38, m	1.35, m [c]	1.29, m [c]	1.44, m 1.33, m	1.30, m [c]
13’	3.50, m	5.39, dd (9.3, 4.3)	1.35, m [c]	1.29, m [c]	1.37, m	1.30, m [c]
14’	1.36, m	2.18, m 2.16, m	1.35, m [c]	1.27, m	3.42, br s	1.27, m
15’	1.36, m	1.51, m	1.31, m	1.29, m	1.44, m 1.37, m	1.30, m
16’	0.88, t (7.1)	3.56, m	1.38, m	0.88, t (7.1)	0.90, t (7.3)	0.89, d (6.7)
17’	-	1.49, m	3.69, dt (10.5, 5.9)	-	-	-
18’	-	0.95, t (7.4)	1.10, d (5.9)	-	-	-
1a	8.21, s	7.98, s	8.21, d (0.9)	8.21, d (1.1)	-	-
4a	6.89, s	6.45, s	6.89, s	6.88, s	-	-
6a	5.74, d (0.9)	5.76, s	5.74, d (0.9)	5.74, d (1.1)	-	-
11a	1.68, s	1.69, s	1.68, s	1.68, m	-	-
12a	7.02, d (15.3)	6.59, d (15.3)	7.01, d (15.2)	7.04, d (15.1)	-	-
13a	8.05, dd (15.3, 11.8)	8.01, dd (15.3, 11.7)	8.05, dd (15.2, 11.6)	8.05, dd (15.1, 11.8)	-	-
14a	7.54, d (11.8)	7.02, d (11.7)	7.54, br d (11.6)	7.56, d (11.8)	-	-
3a’	6.24, d (2.4)	6.18, d (2.2)	6.23, d (2.4)	6.23, d (2.4)	-	-
5a’	6.36, m	6.21, d (2.2)	6.36, d (2.4)	6.36, m	-	-
7a’	2.61, m	2.61, m	2.61, s	2.61, s	-	-
2a’-OH	10.74, s	10.75, s	10.74, s	10.74, s	-	-
4a’-OH	9.24, s	n/a [d]	9.26, s	9.24, s	-	-
misc.	13‘-OH 3.22, d (5.4)	16’-OH n/a [d]	17’-OH 3.31, d (4.7)	13-OH 3.92, d (4.7)	14‘-OH n/a [d]	-

[a] acetone-*d*6. [b] $CDCl_3$. [c] signals could not be unambiguously assigned due to overlaps. [d] no signals observed.

10.1002/chem.202003215

Table 2. ^{13}C NMR spectroscopic data of hybridorubrins A–D (**1**–**4**) and fragirubrins F–G (**5**–**6**) [**1**, **3**–**4**, **6**: 175 MHz; **2**, **5**: 125 MHz]. Chemical shifts are expressed in ppm.

Position	**1** [a]	**2** [b]	**3** [a]	**4** [a]	**5** [a]	**6** [b]
1	65.0, CH_2	64.5, CH_2	65.0, CH_2	64.9, CH_2	155.0, CH	153.7, CH
3	166.1, C	165.4, C	166.2, C	167.9, C	159.3, C	157.8, C
4	98.3, CH	96.5, CH	98.3, CH	97.7, CH	111.3, CH	110.8, CH
5	143.4, C	142.1, C	143.4, C	143.6, C	143.1, C	141.9, C
6	129.6, C	129.2, C	129.6, C	129.8, C	107.6, CH	107.5, CH
7	194.6, C	193.8, C	194.6, C	194.6, C	192.6, C	192.8, C
8	85.7, C	84.5, C	85.7, C	85.7, C	85.4, C	84.1, C
9	189.7, C	189.1, C	189.7, C	189.6, C	193.8, C	193.2, C
10	115.6, C [c]	115.2, C	115.6, C	115.4, C	116.0, C	115.2, C
11	22.6, CH3	22.1, CH_3	22.6, CH_3	22.6, CH_3	22.7, CH_3	22.1, CH_3
12	41.5, CH_2	40.9, CH_2	41.5, CH_2	45.4, CH_2	39.9, CH_2	39.4, CH_2
13	68.8, CH	68.2, CH	68.8, CH	45.4, CH_2	68.4, CH	67.5, CH
14	20.4, CH_3	20.2, CH_3	20.4, CH_3	24.0, CH_3	20.0, CH_3	19.9, CH_3
15	170.6, C	170.6, C	170.6, C	-	170.5, C	170.2, C
16	21.2, CH_3	21.3, CH_3	21.2, CH_3	-	21.1, CH_3	21.2, CH_3
1’	172.4, C	172.5, C	172.4, C	172.4, C	172.7, C	173.1, C
2’	33.9, CH_2	33.2, CH_2	33.9, CH_2	33.9, CH_2	33.8, CH_2	33.2, CH_2
3’	25.6, CH_2	24.6, CH_2	25.6, CH_2	25.6, CH_2	25.6, CH_2	24.6, CH_2
4’	29.8, CH_2	28.9, CH_2	29.9, CH_2	29.5, CH_2	29.7, CH_2	28.9, CH_2
5’–7’	30.4, CH_2 [c]	29.1, CH_2 [c]	30.1, CH_2 [c]	30.4, CH_2 [c]	29.8, CH_2 [c]	29.2, CH_2 [c]
8’	30.4, CH_2 [c]	27.2, CH_2	27.9, CH_2 [c]	30.4, CH_2 [c]	30.4, CH_2 [c]	27.2, CH_2 [c]
9’	30.4, CH_2 [c]	130.3, CH	130.6, CH [c]	30.4, CH_2 [c]	30.4, CH_2 [c]	129.9, CH [c]
10’	30.4, CH_2 [c]	127.8, CH	130.6, CH [c]	30.4, CH_2 [c]	30.4, CH_2 [c]	129.9, CH [c]
11’	26.6, CH_2	25.6, CH_2	27.9, CH_2 [c]	30.4, CH_2 [c]	30.4, CH_2 [c]	27.2, CH_2 [c]
12’	38.7, CH_2	128.6, CH	30.1, CH_2 [c]	30.4, CH_2 [c]	26.6, CH_2	29.2, CH_2 [c]
13’	71.2, CH	129.5, CH	30.1, CH_2 [c]	30.4, CH_2 [c]	38.1, CH_2	29.2, CH_2 [c]
14’	40.9, CH_2	23.6, CH_2	30.1, CH_2 [c]	32.7, CH_2	72.9, CH	31.8, CH_2
15’	19.7, CH_2	23.6, CH_2	26.7, CH_2	23.4, CH_2	31.2, CH_2	22.6, CH_2
16’	14.6, CH_3	36.6, CH_2	40.4, CH_2	14.4, CH_3	10.5, CH_3	14.1, CH_3
17’	-	72.9, CH	67.6, CH	-	-	-
18’	-	30.2, CH_2	24.2, CH_3	-	-	-
1a	155.2, CH	153.8, CH	155.4, CH	155.2, CH	-	-
3a	155.4, C	154.4, C	155.2, C	155.5, C	-	-
4a	115.8, CH	114.7, CH	115.8, CH	115.7, CH	-	-
5a	143.0, C	141.9, C	143.0, C	143.1, C	-	-
6a	110.0, CH	109.5, CH	110.0, CH	109.9, CH	-	-
7a	192.3, C	192.6, C	192.3, C	192.3, C	-	-
8a	86.8, C	84.9, C	86.8, C	86.8, C	-	-
9a	192.8, C	192.2, C	192.8, C	192.8, C	-	-
10a	115.6, C [c]	114.5, C	115.6, C	115.6, C	-	-
11a	22.7, CH_3	22.2, CH_3	22.7, CH_3	22.7, CH_3	-	-
12a	135.1, CH	132.9, CH	135.1, CH	135.0, CH	-	-
13a	131.5, CH	131.1, CH	131.5, CH	131.5, CH	-	-
14a	140.2, CH	137.9, CH	140.2, CH	140.0, CH	-	-
1a’	105.0, C	104.5, C	105.0, C	105.0, C	-	-
2a’	166.2, C	165.5, C	164.0, C	166.2, C	-	-
3a’	101.8, CH	101.1, CH	101.8, CH	101.8, CH	-	-
4a’	164.0, C	161.5, C	166.2, C	164.0, C	-	-
5a’	112.7, CH	111.7, CH	112.7, CH	112.7, CH	-	-
6a’	144.9, C	144.7, C	144.9, C	144.9, C	-	-
7a’	24.1, CH_3	24.0, CH_3	24.1, CH_3	24.1, CH_3	-	-
8a’	170.7, C	169.9, C	170.7, C	170.7, C	-	-

[a] acetone-*d*6. [b] $CDCl_3$. [c] signals could not be unambiguously assigned due to overlaps.

10.1002/chem.202003215

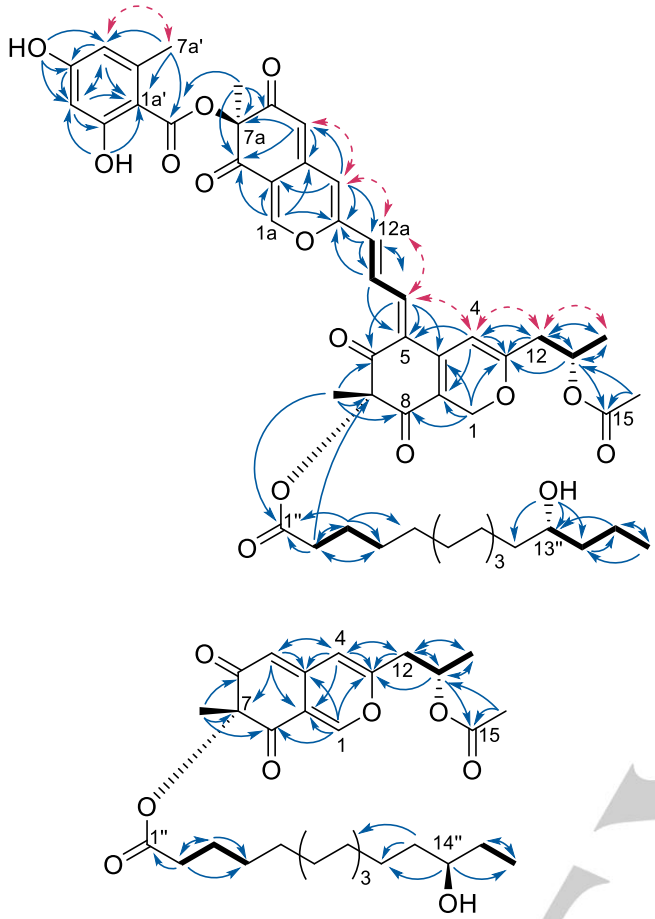

Figure 2: Key NMR correlations of hybridorubrin A (**1**) and fragirubrin F (**5**). Bold bonds: $^{1}H/^{1}H$ COSY correlations; solid, blue arrows: $^{1}H/^{13}C$ HMBC correlations; dashed, pink arrows: $^{1}H/^{1}H$ ROESY correlations.

Stereochemistry of azaphilones occurring in *H. fragiforme* and revision of rutilins C–D

The stereochemistry of the azaphilones, particularly of C-8 in the backbone, is an important aspect of structural complexity. While the first occurrence of (−)-mitorubrins was described in 1965 by Büchi *et al.* from cultures of *Penicillium rubrum* [16] (current name: *Talaromyces ruber*), Steglich *et al*. later described (+)-stereoisomers of mitorubrins from the stromata of *H. fragiforme.*[3] Curiously, the genus *Talaromyces* was reported to contain either (+) or (−)-mitorubrins depending on the species.[17]

We utilized ECD spectroscopy as a means to assess the stereochemistry of the monomeric azaphilones. A study by Clark *et al.* on chemical synthesis of the azaphilone backbone[18] allowed for relatively simple assignment: mitorubrinol **8** from *H. fragiforme* showed a positive cotton effect (CE) at 245 nm, as well as a negative CE at 226 and 272 nm (Figure S44). These ECD data indicate an (*S*)-(+)-configuration,[18] which we conferred to all mitorubrin-type azaphilones from *H. fragiforme* due to their common biosynthetic origin (see Biosynthesis section for details). However, all fragirubrins[1b] (Figure S44) showed inverted ECD spectra with positive CE at *ca.* 230 and 274 nm and negative CE at *ca.* 250 nm, accordingly rendering them *(R)*-(−)-isomers.

Taking the ECD results and the biosynthetic gene cluster (BGC) analysis (see Biosynthesis section below) into account then allows for stereochemical assignment of the hetereodimers: rutilins like **12**–**13**, which consist of two (*S*)-mitorubrin-type building blocks, are hence (*S*)-configured at both C-8 and C-8a. Hybridorubrins **1**–**4**, in turn, are (*S*)-configured at C-8a in their mitorubrin moiety and *(R)*-configured at C-8 in their fragirubrin part. We hence have to revise data from our prior study with rutilins C–D **12**–**13** (and the mitorubrins) [1b] to be (*S*)-configured at C-8 and C-8a.

Bioactivity testing

Compounds **1**–**2**, **4**–**10**, and **12**–**18** were tested for their antimicrobial activity in a minimum inhibitory concentration (MIC) assay as well as for their cytotoxicity, but were found to be devoid of activity against the examined test organisms or cell lines (Table S3). The lack of antimicrobial and cytotoxic activities are largely in accordance with former findings for mitorubrin-type azaphilones.[4]

In addition, **1**–**4**, **7**–**10**, and **14**–**15** were tested for their inhibitory effect on biofilm formation of *Staphylococcus aureus* (Table 3). It has to be noted that due to minor impurities in the samples, the given percentage values only allow for a rough estimation of bioactivity. Strong activity was observed for the bisazaphilones hybridorubrins A **1**, C **3**, D **4**, and rutilin C **12**. These compounds possessed potency similar to the reference compound microporenic acid A,[19] as well as sclerin and sclerin diacid from *H. fragiforme.*[8] The mitorubrin-type azaphilones **7** and **9**, as well as the fatty acid-containing **15** showed weak activity, while **8**, **10**, and **14** showed no inhibition.

These results allow for preliminary structure-activity relationships (SAR) to be deduced: since rutilin C **12** showed much stronger inhibition of biofilm formation than **7**, a strong influence of the fused second azaphilone backbone is suggested. In addition, the differing biofilm formation inhibition of the mitorubrin-type azaphilones **7**–**10** indicates a modest influence of the functional group at C-14: a methyl group or an acetate unit (**7**, **9**) allowed for weak activity, while azaphilones carrying more polar hydroxyl or carboxylic acid moieties at C-14 (**8**, **10**) exhibited no biofilm formation inhibition.

Lenormandin F **14** and fragirubrin A **15**, which both carry a C_{16} fatty acid moiety instead of an orsellinic acid residue at C-8, only differ in the presence of an acetate moiety at C-13 in **15**. While **14** showed no activity, **15** exhibited weak activity similar to **7** and **9**. Hence, a positive effect of C-13 acetylation unit can be deduced. By comparing **7** and **9** to **15**, the presence of an orsellinic acid or a fatty acid moiety at C-8 does not seem to be highly relevant for activity against *S. aureus* biofilm formation.

Taking these findings into account, the strong bioactivity which was measured for hybridorubrins A **1**, C **3**, D **4** and rutilin C **12** can be mainly explained by the fusion of two azaphilone building blocks. As acetylation of C-13 was deduced to be beneficial for bioactivity, **4** consequently exhibited a weaker effect than **1** and **3**.

Table 3. Inhibitory effect of azaphilones from *Hypoxylon fragiforme* on biofilm formation of *Staphylococcus aureus*.

compound	biofilm inhibition /% [a]	concentration /µg×mL^{-1}	potency of inhibition [b]
hybridorubrin A (**1**)	81	250	+++
	72	125	
	68	62.5	
	61	31.3	
	45	15.6	
	32	7.8	
	27	3.9	
hybridorubrin C (**3**)	82	250	+++
	79	125	
	65	62.5	
	60	31.3	
	60	15.6	
	34	7.8	
	25	3.9	
hybridorubrin D (**4**)	71	250	+++
	61	125	
	50	62.5	
	37	31.3	
	27	15.6	
mitorubrin (**7**)	29	250	+
	27	125	
	27	62.5	
mitorubrinol (**8**)	n.i.	250	−
mitorubrinol acetate (**9**)	24	250	+
mitorubrinic acid (**10**)	n.i.	250	−
rutilin C (**12**)	59	250	+++
	72	125	
	63	62.5	
	51	31.3	
	41	15.6	
lenormandin F (**14**)	n.i.	250	−
fragirubrin A (**15**)	27	250	+
	29	125	
	38	62.5	
microporenic acid A (reference) [19]	81	250	+++
	83	125	
	45	62.5	
	20	31.3	

[a] only inhibition values ≥20% depicted here, n.i.: no inhibition. [b] +++: inhibition ≥70%; ++: inhibition ≥40 and <70%; +: inhibition ≥20 and <40%; −: inhibition <20%

Azaphilone biosynthetic gene cluster (BGC) analysis

In order to understand how the wide diversity of azaphilone-type compounds in the stromata of *H. fragiforme* is genetically encoded, we investigated the genome sequence of the producer organism. Genome sequencing of the fungus had been performed in the context of a previous study.[9]

To identify a likely candidate gene cluster, the previously published sequences of the biosynthetic gene clusters (BGC) encoding azaphilones in *Monascus ruber* [20] (*i.e.* monascin, ankaflavin and monascorubrin), azanigerones in *Aspergillus niger* [21] and mitorubrinol in *Talaromyces marneffei* [22] were used for homology searches. In *M. ruber*, *A. niger* and *T. marneffei* assembly of the azaphilone core structure is initiated by the action of a non-reducing polyketide synthase (NR-PKS) and finalized by subsequent processing of a ketoreductase (KR) and FAD-dependent monooxygenase (FAD-MO).[20] These three core proteins were used initially as the template for BLASTP searches against a *H. fragiforme* protein database created using the software Geneious 9.1.8.

In total, seven NR-PKS-containing BGC were found. However, only one included the required KR and FAD-MO encoding genes. This BGC (designated as *hfaza1*, GenBank Acc. No. MN736721) is composed of seven genes, the majority of which show high homology with the biosynthetic genes of the *M. ruber* azaphilone *mrPig* and the *T. marneffei* mitorubrinol biosynthetic gene clusters (Figure 3). In addition to the NR-PKS (*hfaza1A*), the ketoreductase (*hfaza1F*) and the FAD-dependent monooxygenase (*hfaza1D*), genes encoding an NADPH-dependent dehydrogenase (*hfaza1B*), an ac(et)yltransferase (*hfaza1E*), a transporter (*hfaza1C*) and a transcription factor (*hfaza1G*) are present.

A previous investigation of the mitorubrinol gene cluster in *T. marneffei* showed that two PKS genes are involved in the biosynthesis of **8** and **10**.[22] The second PKS encodes the biosynthesis of orsellinic acid. We therefore searched for a homologue of the putative *T. marneffei* orsellinic acid synthase (OSAS) *pks12* in *H. fragiforme*. Accordingly, we found a gene cluster encoding a highly similar NR-PKS together with a set of genes of which the majority also appeared in the *M. ruber* (Figure 3) and *A. niger* azaphilone biosynthetic gene clusters. This second gene cluster is designated as *hfaza2* (GenBank Acc. No. MN736720). The respective NR-PKS (Hfaza2A) has an SAT-KS-AT-PT-ACP domain structure, thus lacking a typical C-terminal release domain. Additional genes in the *hfaza2* BGC encode: an FAD-dependent monooxygenase (*hfaza2D*) with high homology to *hfaza1D* and *mrPigN*; an ac(et)yltransferase (*hfaza2E*) homologous to *hfaza1E* and *mrPigD*; a P450 monooxygenase (*hfaza2F*); and an NADPH-dependent dehydrogenase with homology to *hfaza1B* and *mrPigH*. Furthermore, two similar genes were also found in the BGC (*hfaza2B* and *hfaza2C*) that did not produce any hits in BLASTP searches against the Swiss-Prot database, but showed strong homology with the azaphilone biosynthesis genes *mrPigM* and *mrPigO* from *M. ruber*. Based on knockout experiments of the two latter, it was deduced that MrPigM is an acetyltransferase, whereas MrPigO performs deacetylation.[20] In addition to these genes, two FAD-dependent oxidoreductases (*hfaza2J* and *hfazaM*) were found, which are very similar to *azaG* and *azaL*, both of which are part of the azanigerone biosynthetic pathway.[21]

10.1002/chem.202003215

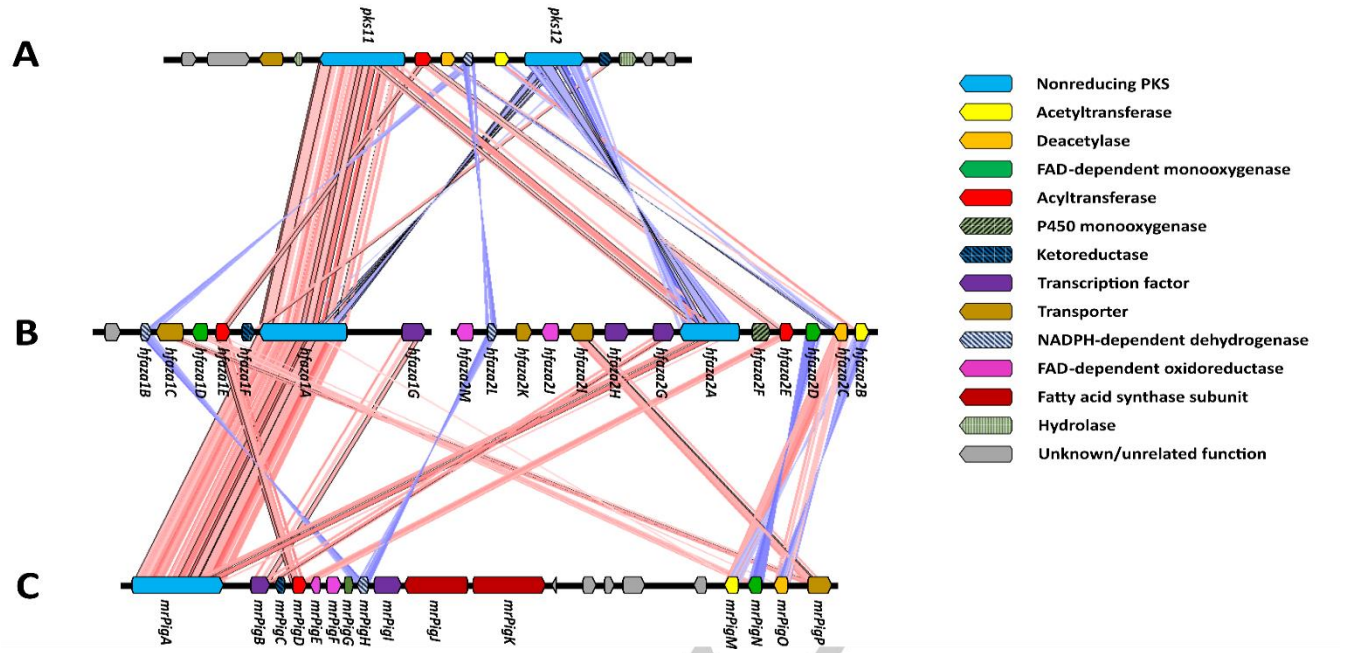

Figure 3. Biosynthetic gene cluster (BGC) comparison of the putative azaphilone producing clusters using the Artemis comparison tool (ACT): **A**, the known mitorubrin BGC of *T. marneffei*; **B**, *Hfaza1* and *Hfaza2* from *H. fragiforme*; **C**, the known *MrPig* BGC from *M. ruber*. In accordance with the original publication,[22] no further labels were assigned to the *T. marneffei* genes. Homologous gene regions are connected by red lines indicating identical orientations and blue lines implying gene inversion.

Finally, two putative transcription factors (*hfaza2G* and *hfaza2H*) and two putative transporters (*hfaza2I* and *hfaza2K*) were also assigned to the cluster. A detailed comparison of the *hfaza1* and *hfaza2* clusters with the uncharacterized mitorubrinol BGC reported from *T. marneffei* [22] showed the presence of almost all genes from the latter in the *H. fragiforme* BGC (Figure 3). Homologs of Hfaza1A, Hfaza2A, Hfaza1B, Hfaza1E, Hfaza1F, Hfaza2L, Hfaza2E, Hfaza2C and HfazaB were found. The *T. marneffei* cluster is expanded by two hydrolase enzymes, but no FAD-dependent monooxygenase, P450 monooxygenases, FAD-dependent oxidoreductases and transcription factors are present. Therefore, we propose, according to the homology analyses, that two unlinked BGC (*Hfaza1* and *Hfaza2*) act together in order to assemble and diversify azaphilones in *H. fragiforme*.

H. fragiforme does not readily produce azaphilones in laboratory culture, so it is not yet possible to investigate the biosynthesis experimentally. However, there is now sufficient detailed knowledge concerning the biosynthesis of related compounds in other organisms to allow the development of a detailed biosynthetic hypothesis based on the combination of structure information and analytical HPLC-MS data (Scheme 1).

The formation of azaphilones likely starts in a similar fashion as proved for azanigerones and *Monascus* pigments with the NR-PKS Hfaza1A producing a hexaketide chain, which is subsequently cyclized by the product template domain and released by the reductive release domain of the PKS to yield the reactive benzaldehyde intermediate **20**. Chen *et al.* reported that in *M. ruber* ketoreduction at C-13 is required prior to hydroxylation at C-8 to afford the pyran ring.[20] In the crude stromatal extracts of *H. fragiforme* we could not find any evidence for the existence of such a bicyclic pyranoquinone intermediate **22**. Instead, we found a conspicuous peak with m/z = 249 $[M+H]^+$, which displayed fragmentation patterns, a UV/vis spectrum, and molecular formula consistent with the putative keto-intermediate **21** (Tables S4−S5). We therefore conclude, that **21** might be produced by hydroxylation of **20** at C-8 by the FAD-dependent monooxygenase Hfaza1D and subsequent spontaneous pyran ring formation. As Hfaza2D also encodes a homologous enzyme there is a possibility that it can perform the same reaction. In a previous study based on crystal structure data and quantum mechanical/molecular mechanical calculations of the homologous FAD-dependent monooxygenase TropB, it has been demonstrated that such enzymes govern a highly enantioselective transformation.[23] The occurrence of the homologous pair Hfaza1D/Hfaza2D would therefore be consistent with the observation of different stereoconfigurations at C-8 between mitorubrin-type and fragirubrin-type azaphilones. Compound **21** can then be further processed by the ketoreductase Hfaza1F to yield **22**. As previously stated, we could not detect **22**, which can be possibly explained by differences in metabolic rates due to differences in enzyme reaction rates or expression levels of *hfaza1F* and subsequent processing enzymes.

10.1002/chem.202003215

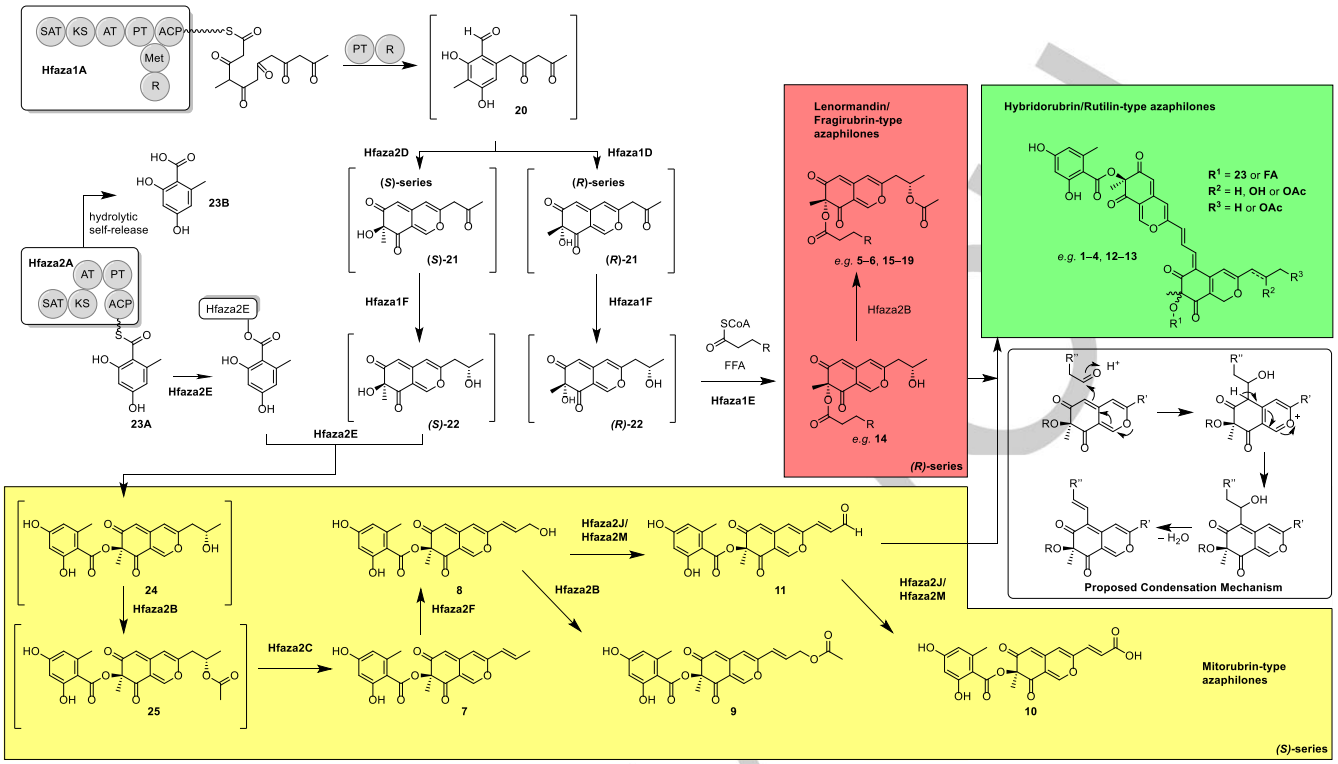

Scheme 1: Biosynthetic hypothesis for the production and diversification of azaphilone-type compounds in *H. fragiforme*. Putative intermediates that could not be isolated and were only detectable in traces by HPLC-MS or not detectable at all are shown in square brackets. R in the free fatty acids (FFA) and respective side chain indicates variations in chain length, hydroxylation and unsaturation pattern depending on the final product.

In the next step, the pathway branches into two directions depending on the attached side chain. In order to yield lenormandin-type azaphilones (such as **14**) the backbone **22** can undergo acylation at the C-8 alcohol mediated by the acyltransferase Hfaza1E. Subsequent acetylation at the C-13 alcohol by the putative acetyltransferase Hfaza2B will lead to the highly diverse group of fragirubrins (**5**−**6**, **15**−**19**), which differ among each other in the chain length, desaturation level and hydroxylation pattern of the side chain. This side chain very likely originates from different free or CoA-bound fatty acids of the primary metabolism implying a broad substrate tolerance of Hfaza1E. Acyltransferases accepting a wide range of enzyme-free acyl substrates are also involved in the biosynthesis of squalestatin.[24] As only lenormandin F **14** has been isolated as a representative of this type of compounds from *H. fragiforme*, we assume that the majority of lenormandins are transformed into the respective fragirubrins. This hypothesis is consistent with observations made in *H. lenormandii*, which only produces the azaphilones named after this fungus.[12] Thus, it can be speculated that *H. lenormandii* lacks homologues of Hfaza2B.

The diversity of mitorubrin-type azaphilones likely starts by the attachment of orsellinic acid **23** to the hydroxyl group at C-8 catalysed by Hfaza2E leading to the intermediate **24**. Due to the structural differences between **24** and fatty acids it seems unlikely that transfer reactions are conducted by the very same enzyme. Hence, we expect the acyltransferases from both clusters to be specific for different types of substrates. In addition, we assume that these enzymes are also highly stereoselective concerning the substrate **22** as only a single enantiomer for each compound can be detected.

Due to the absence of another obvious OSAS encoded in the genome, the involvement of Hfaza2A in the synthesis of **23** seems most likely. This is also supported by the strong homology of Hfaza2A to PKS12 of the mitorubrinol BGC in *T. marneffei*. The latter enzyme was shown to be crucial for mitorubrinol **8** [25] and mitorubrinic acid **10** [25] biosynthesis by knock-down experiments in the producing fungus, but the actual function could not be deduced from the data. Hence, it was speculated that PKS12 might be responsible for orsellinic acid biosynthesis. Unfortunately, the authors only looked specifically for the absence of **8** and **10**, but did not search for additional products in the extracts of their transformants to confirm this idea.[22]

The lack of a release domain in the proposed OSAS Hfaza2A could be compensated by the acyltransferase Hfaza2E, which might directly load the ACP-bound **23A**. Such reaction has already been suggested for the acyltransferase MrPigD, which presumably accepts ACP-bound fatty acids in *Monascus* pigment biosynthesis [20] and has been well characterized for the acyltransferase LovD involved in lovastatin biosynthesis.[26] Because **23B** can also be detected as free acid in the stromatal crude extracts, we expect a hydrolytic self-release mechanism analogously to truncated forms of the methylorcinaldehyde synthase.[27] Intermediate **24** is then acetylated by the putative acetyl transferase Hfaza2B to give **25**. Mass searches for the

compounds **24** and **25** revealed the presence of respective traces in the stromatal crude extracts (Table S5). Because of the very low amount of compound the corresponding relationships can however not be verified. The following step might involve deacetylation carried out by Hfaza2C to yield the mitorubrin **7**, which in return is hydroxylated at C-14 putatively by the P450 monooxygenase Hfaza2F in order to afford one of the major stromatal metabolites, mitorubrinol **8**.

Mitorubrinol **8** then acts as the starting material for the biosynthesis of **9** through the acetylation of the C-14 alcohol performed either by Hfaza2B or a cluster independent acetyltransferase. In addition, **8** is also likely to be an intermediate towards mitorubrinic acid **10** *via* the formation of the aldehyde mitorubrinal **11**. We found a corresponding peak in stromatal crude extracts exhibiting the expected mass spectra (Figure S2, Tables S4−S5). We were unable to isolate this compound, but semi-synthetically obtained standards of **11** by oxidation of **8** with manganese oxide proved that the observed peak is indeed **11**.

The respective biosynthetic steps to **10** might be carried out by the action of the FAD-dependent oxidoreductases Hfaza2J and Hfaza2M. As the *T. marneffei* BGC also encodes the production of **10**, but lacks oxidoreductase genes, a different mechanism is also possible. Interestingly, the mitorubrinol cluster of *T. marneffei* only leaves limited options to explain the conversion of **11** into **10**. The function of the highly conserved NADPH-dependent dehydrogenase still remains obscure in all azaphilone biosynthetic pathways. Hence, it could theoretically also be involved in such oxidation steps.

Finally, we propose that the aldehyde functionality of **11** acts as an electrophile for the nucleophilic C-6 in all *H. fragiforme* monomeric azaphilones to afford dimers of the rutilin (**12**−**13**)- and hybridorubrin-type (**1**−**4**), as already postulated by Quang *et al.* for rutilins A and B.[28] The presence of rutilins in *Hypoxylon rutilum* as major stromatal metabolites could also indicate that condensation is enzyme-catalyzed.[28] However, this phenomenon could also be explained by the lack of an FAD-dependent oxidoreductase to prevent the biosynthesis of a carboxylic acid functionality leaving the reactive aldehyde as the final enzymatic product. This is also consistent with the observation that no carboxylated azaphilones have been detected in *H. rutilum*.[28] On the other hand, the mechanism could also involve radicals. The structures of the known bisazaphilone diazaphilonic acid [29] or the azaphilone derived nitrogen-containing chaetoglobins [30] (Figure S3) might be formed by a possible recombination of radicals establishing the carbon-carbon bond connecting the substructures.

When comparing the biosynthetic machinery of mitorubrins in *H. fragiforme* and *T. marneffei* various questions remain. The lack of monooxygenase genes in the cluster of the latter would prevent backbone assembly. Furthermore, monooxygenases are also very likely required to obtain mitorubrinol **8**. It seems therefore likely that enzymes encoded outside of the BGC participate in the azaphilone formation of *T. marneffei*. Based on our biosynthetic hypothesis, we propose that the production of lenormandin-type azaphilones requires only genes from *Hfaza1* and thus is likely evolved earlier in these fungi. Consequently, *Hfaza2* might be acquired later, *e.g.* by horizontal gene transfer from *T. marneffei* or related fungi and has proved for the fungus to be compatible with *Hfaza1*.

The existence of intertwining secondary metabolite gene clusters has already been reported for the production of the structurally distant compounds fumagillin and pseurotin A in *Aspergillus fumigatus*.[25] However, these clusters were physically linked and consequently translocation of genes into neighbouring BGC can be explained by simple inversion of certain genomic regions within such a supercluster. Recently, independent gene clusters have been demonstrated to be responsible for the formation of the azaphilone azasperpyranone A in *Aspergillus terreus*. While one BGC produced the azaphilone backbone, the other BGC afforded and processed 5-methyl orsellinic acid (5-MOA). The respective 5-MOA PKS contained a methyltransferase (MeT) and thiolesterase (TE) domain and shared only little homology with Hfaza2A.

In addition to the elucidation of the biosynthetic pathway of azasperpyranone A, the regulatory network of the participating BGCs was deciphered by gene knockout of the encoded transcription factors (TF) and gene expression analysis. It was shown that each BGC is upregulated by a cluster-specific TF, which in return are regulated by a third TF located in one of the BGC.[31] The regulatory network for azaphilone production in *H. fragiforme* could be highly similar as three TFs have been identified across *hfaza1* and *hfaza2*. We thus tried to experimentally link *Hfaza1* and *Hfaza2* with the known azaphilones by ectopic overexpression of the individual TF genes using previously described methods.[32] However, this proved unsuccessful. Knock-out strategies are not viable in the Hypoxylaceae as azaphilones are exclusively formed during stromatal development, which cannot be induced under laboratory conditions.

We could also find highly similar homologs of the two clusters in the taxonomically related fungus *H. rickii* and the more distantly related *H. rubiginosum* (data not shown), which are known to produce mitorubrins and/or the closely-related rubiginosins.[33] This observation further supports our theory about azaphilone biosynthesis in *H. fragiforme* and enables further options to study the pathways in detail. However, it will be a special challenge to obtain final proof of the biosynthetic mechanism because the stromata can presently not be grown in the laboratory, and hence the only path forward would be heterologous expression.

Conclusions

We used a combination of classical natural product chemistry and state-of-the-art genome sequencing to deduce the biosynthesis of azaphilone pigments in *H. fragiforme*, demonstrating the powerful combination of those two methods.

We showed that both possible C-8 stereoisomers of azaphilones are produced in the stromata, which allows for an assignment to subgroups: (1) the C-8(*R*)-configured azaphilones consists of the acyl-carrying lenormandins and fragirubrins; (2) the group of C-8(*S*)-configured azaphilones carry an orsellinic acid moiety and belong to the family of mitorubrins, and their fusion products, rutilins; and (3) the novel hybridorubrins, which

are of mixed stereochemistry, as their building blocks originate from groups (1) and (2). Furthermore, the hybridorubrins A **1**, C **3**, and D **4** exhibited a strong bioactivity against formation of *S. aureus* biofilms.

Examination of the *H. fragiforme* genome revealed two biosynthetic gene clusters (BGC) to be most likely responsible for biosynthesis of azaphilone polyketides. The *hfaza1* BGC is likely to be responsible for biosynthesis of the azaphilone backbone as well as addition of fatty acid moieties to yield group 1 compounds. In parallel, the *hfaza2* BGC synthesizes orsellinic acid which is esterified to the backbone to yield group 2 azaphilones and tailors the gained mitorubrins to obtain a high diversity of derivatives. We suggest a spontaneous aldol condensation reaction to be responsible for the formation of hybridorubrin and rutilin bisazaphilones from reactive aldehyde intermediates in *H. fragiforme*, which however needs experimental verification. These results reveal the first example of two distant, cross-acting BGC that enable a large diversity of azaphilone products through natural mix-and-match strategies.

Experimental Section

General

NMR spectra were recorded with an Avance III 700 spectrometer with a 5 mm TCI cryoprobe (^{1}H 700 MHz, ^{13}C 175 MHz) and an Avance III 500 spectrometer (^{1}H 500 MHz, ^{13}C 125 MHz) (both Bruker, Billerica, MA/USA). Optical rotations were taken with a MCP 150 polarimeter (Anton Paar, Graz, Austria) and UV spectra with a UV-2450 UV/vis spectrophotometer (Shimadzu, Kyoto, Japan). IR spectra were taken with a Spectrum 100 FT-IR spectrometer (Perkin Elmer, Waltham, MA/USA).

ESI-MS spectra were recorded with an UltiMate® 3000 Series uHPLC (Thermo Fisher Scientific, Waltman, MA/USA) utilizing a C18 Acquity® UPLC BEH column (2.1×50 mm, 1.7 µm; Waters, Milford, USA) connected to an amaZon speed® ESI-Iontrap-MS (Bruker, Billerica, MA, USA). HPLC parameters were set as follows: solvent A: H_2O+0.1% formic acid, solvent B: acetonitrile (ACN)+0.1% formic acid, gradient 5% B for 0.5 min, increasing to 100% B in 19.5 min, keeping 100% B for further 5 min, flowrate 0.6 mL×min^{-1}, and DAD detection 190−600 nm.

HR-ESI-MS spectra were obtained with an Agilent 1200 Infinity Series HPLC (Agilent Technologies, Böblingen, Germany; conditions same as for ESI-MS spectra) connected to a maXis® ESI-TOF-MS (Bruker).

Fungal material and extraction

To generate crude extract (1), air-dried stromata (fruiting bodies, *ca.* 65 g) of *Hypoxylon fragiforme* were collected in 2017 from *Fagus sylvatica* in the vicinity of Braunschweig, Germany, by Lucile Wendt. Extraction was performed by adding 500 mL acetone, followed by ultrasonication at 40 °C for 1 h. This procedure was repeated twice. The extracts were combined and dried *in vacuo*, which led to approx. 6 g of crude extract (1). For the second crude extract (2), *ca.* 25 g of air-dried stromata of *Hypoxylon fragiforme* were collected in 2016 from *Fagus sylvatica* in the vicinity of Lake Starnberg, Germany, by Lucile Wendt. Extraction was performed as described above. This yielded *ca.* 3 g of crude extract (2).

Isolation of secondary metabolites 1−6

The first crude extract (1) yielded hybridorubrins A–B (**1**–**2**) and fragirubrins F−G (**5**−**6**), while hybridorubrin C–D (**3**–**4**) could be detected but not isolated to purity. Thus, the second extract (2) was utilised to isolate **3** and **4**, while **1** was isolated again as a by-product.

Initially, the first crude extract (1) was separated by a Reveleris® X2 Flash Chromatography system (Büchi, Essen, Germany). A 40 g silica cartridge (120×30 mm, 40 µm, SN 145146132, W.R. Grace, Columbia, MD/USA) was loaded with the crude extract and eluted with a ternary gradient (solvent A: DCM, B: DCM:acetone 9:1, C: acetone) as follows: at a flow rate of 40 mL×min^{-1}, isocratic conditions at 100% A were set for 4 min, followed by a gradient to 100% B in 25 min. This was followed by an increase of solvent C to 100% in 20 min. This led to six fractions (t_R fraction I: 3.4−14.3 min, II: 14.7−15.9 min, III: 16.6−20.4 min, IV: 21−25.4 min, V: 26−29.8 min, VI: 30.3−52.2 min), which were evaporated to dryness *in vacuo* at 40°C.

Fractions I, II, and V (see subsequent paragraphs) were further processed using a preparative HPLC system (Gilson, Middleton, WI/USA; GX-271 Liquid Handler with a GX Direct Injection Module, DAD 172, 305 and 306 Pump, 806 Manometric Module 811D Dynamic Mixer, 402 Syringe Pump). A Nucleodur C18ec column (150×40 mm, 7 µm; Macherey-Nagel, Düren, Germany) was used at a flow rate of 40 mL×min^{-1} using solvent A: H_2O+0.1% formic acid and solvent B: ACN+0.1% formic acid. After evaporation of ACN *in vacuo*, the aqueous residues were frozen and freeze-dried using an Alpha 1-4 LSC freeze dryer (Christ, Osterode, Germany): Fraction I (2×70 mg) and II (3×100 mg) were separated with a gradient using isocratic conditions for 5 min at 60% B, followed by an increase to 100% B in 45 min, 5 min of isocratic conditions and, ultimately, a decrease to 60% B in 2 min. Fragirubrin G (**6**, 0.9 mg) was gained from fraction I, while fragirubrin F (**5**, 21.6 mg) was isolated from fraction II. Fraction V (1×100 mg) was separated using a gradient from 45 to 80% B in 40 min, followed by an increase to 100% B in 5 min and isocratic conditions at 100% B for 15 min. It yielded hybridorubrin B (**2**, 2.8 mg). Fraction VI (1×40 mg) was separated on a RP-MPLC system (Kronlab, Sinsheim, Germany; column 480×30 mm, ODS/AQ C18, solvents as described for fractions I−V) at a flow rate of 30 mL×min^{-1}. Starting with isocratic conditions at 10% B for 5 min, a gradient to 100% B in 60 min was followed by isocratic conditions at 100% B for 30 min. Hybridorubrin A (**1**, 4.1 mg) was obtained from this separation.

The second crude extract (2) was separated using the aforementioned Reveleris® X2 flash chromatography system. A 120 g C18 cartridge (200×40 mm, 40 µm, SN 5152991, Grace) was loaded with the crude extract and eluted with a binary gradient (solvent A: H_2O+0.1% formic acid; solvent B: ACN+0.1% formic acid) as follows: flow rate: 80 mL×min^{-1}, isocratic conditions at 5% B for 3 min, followed by an increase to 45% B in 1 min. This was followed by an increase to 80% B in 10 min. Subsequently, the gradient was increased to 100% B in 25 min. This was kept for further 20 min. This yielded fractions I (t_R: 40−45 min) and II (52.5−70 min). Both, fractions I (1×180.3 mg) as well as II (1×122 mg), were individually processed *via* manual NP column chromatography. For this, the material was adsorbed to Silica bulk material (63−200 µm) and transferred to a Loading Cartridge (SN 8634349, Grace). Downstream of that, a 12 g Silica cartridge (SN 5146131, Grace) was installed. Applying a vacuum of *ca.* 50 mbar, the extract was separated using the following solvents: A: *n*-heptane, B: DCM, C: MeOH. A step-gradient using 100 mL of the following solvent mixtures was gradually applied: (i) 20:80:0 (% A:B:C, v/v/v), (ii) 0:100:0, (iii) 0:99:1, (iv) 0:98:2, (v) 0:96:4, (vi) 0:93:7, (vii) 0:90:10, (viii) 0:85:15, (ix) 0:80:20. Each solvent mixture was loaded onto the device and the eluent gathered before another step was applied. Hence, chromatographic separation of fraction I yielded fraction (v), while fraction

II yielded fractions (vi) and (vii), which were combined. Fraction (v) (2×10.5 mg) was further separated using a PLC 2250 HPLC system (Gilson) equipped with an X-Bridge C18 column (250×19 mm, 5 µm, Waters), the solvents A: H_2O+0.1% formic acid and B: ACN+0.1% formic acid, and the following gradient: flow rate: 20 mL×min^{-1}, isocratic conditions at 40% B for 5 min, followed by an increase to 75% B in 5 min. This was followed by an increase to 100% B in 50 min. This yielded hybridorubrin D (**4**, 1.7 mg). Fraction (vi+vii) (8×11 mg) was separated using the PLC 2250 with the conditions as described above. First, isocratic conditions at 40% B were applied for 5 min, followed by an increase to 75% B in 5 min. Then, 75% B were kept for 25 min. Same fractions of the eight separations were combined according to LCMS results, which yielded hybridorubrin A (**1**, 11.9 mg) and a yet impure hybridorubrin C (**3**). The latter (1×4.7 mg) was further purified using again the PLC 2250 with the same conditions as before, but with the exception of applying 77% instead of 75% B. This yielded hybridorubrin C (**3**, 1.7 mg).

Physicochemical data

Hybridorubrin A **1**: yellow oil; $[\alpha]_D$ = +340 (*c* 0.02, ACN); ^{1}H NMR (acetone-*d*6, 700 MHz): see Table 1; ^{13}C NMR (acetone-*d*6, 175 MHz): see Table 2; IR (ATR): ν_{max} = 2927, 2854, 1717, 1621, 1261 cm^{-1}, see Figure S42; UV/vis (acetone): λ_{max} (ε) = 215 (4.54), 268 (4.40), 360 (4.60), 441 (4.37) nm; ECD (ACN) $\lambda(\Delta\varepsilon)$: 231 (−5.0), 265 (−0.6), 293 (−5.4), 360 (+5.3) nm, see Figure S43; ESI-MS: *m/z* 927.58 $[M+H]^+$, 925.55 $[M-H]^-$; HR-ESI-MS: *m/z* 927.4163 $[M+H]^+$ (calcd. for $C_{52}H_{63}O_{15}$, 927.4161); t_R = 16.3 min.

Hybridorubrin B **2**: yellow oil; $[\alpha]_D$ = +580 (*c* 0.02, ACN); ^{1}H NMR ($CDCl_3$, 500 MHz): see Table 1; ^{13}C NMR ($CDCl_3$, 125 MHz): see Table 2; IR (ATR): ν_{max} = 2929, 2855, 1717, 1630, 1263 cm^{-1}, see Figure S42; UV/vis (ACN): λ_{max} (ε) = 213 (4.50), 268 (4.37), 362 (4.52), 441 (4.31) nm; ECD (ACN) $\lambda(\Delta\varepsilon)$: 198 (+5.4), 231 (−8.9), 267 (−1.7), 290 (−8.7), 355 (+8.0) nm, see Figure S43; ESI-MS: *m/z* 951.49 $[M+H]^+$, 949.48 $[M-H]^-$; HR-ESI-MS: *m/z* 951.4154 $[M+H]^+$ (calcd. for $C_{54}H_{63}O_{15}$, 951.4161); t_R = 16.4 min.

Hybridorubrin C **3**: yellow oil; $[\alpha]_D$ = +355 (*c* 0.02, ACN); ^{1}H NMR (acetone-*d*6, 700 MHz): see Table 1; ^{13}C NMR (acetone-*d*6, 175 MHz): see Table 2; IR (ATR): ν_{max} = 2930, 2855, 1717, 1630, 1263 cm^{-1}, see Figure S42; UV/vis (ACN): λ_{max} (ε) = 215 (4.4), 269 (4.2), 364 (4.4), 443 (4.1) nm; ECD (ACN) $\lambda(\Delta\varepsilon)$: 197 (−7.2), 206 (−3.1), 213 (−8.3), 218 (−2.2), 232 (−12.7), 267 (+1.7), 289 (−11.0), 352 (+8.9) nm, see Figure S43; ESI-MS: *m/z* 953.52 $[M+H]^+$, 951.48 $[M-H]^-$; HR-ESI-MS: *m/z* 953.4321 $[M+H]^+$ (calcd. for $C_{54}H_{65}O_{15}$, 953.4318); t_R = 16.6 min.

Hybridorubrin D **4**: yellow oil; $[\alpha]_D$ = +173 (*c* 0.015, ACN); ^{1}H NMR (acetone-*d*6, 700 MHz): see Table 1; ^{13}C NMR (acetone-*d*6, 175 MHz): see Table 2; IR (ATR): ν_{max} = 2924, 2854, 1721, 1622, 1262 cm^{-1}, see Figure S42; UV/vis (ACN): λ_{max} (ε) = 214 (4,36), 266 (4.11), 337 (4.12) nm; ECD (ACN) $\lambda(\Delta\varepsilon)$: 209 (+2.6), 228 (−2.4), 268 (−0.5), 296 (−4.5), 330 (+2.7) nm, see Figure S43; ESI-MS: *m/z* 869.43 $[M+H]^+$, 867.39 $[M-H]^-$; HR-ESI-MS: *m/z* 869.4110 $[M+H]^+$ (calcd. for $C_{50}H_{57}O_{14}$, 869.4107); t_R = 18.7 min.

Fragirubrin F **5**: yellow oil; $[\alpha]_D$ = −10 (*c* 0.1, ACN); ^{1}H NMR (acetone-*d*6, 500 MHz): see Table 1; ^{13}C NMR (acetone-*d*6, 125 MHz): see Table 2; IR (ATR): ν_{max} = 2925, 2854, 1737, 1715, 1639, 1233 cm^{-1}, see Figure S42; UV/vis (ACN): λ_{max} (ε) = 220 (4.18), 326 (4.22) nm; ECD (ACN) $\lambda(\Delta\varepsilon)$: 199 (−8.1), 232 (+1.9), 248 (−1.6), 273 (+5.2), 323 (−5.3) nm, see Figure S44; ESI-MS: *m/z* 547.34 $[M+H]^+$, 545.28 $[M-H]^-$; HR-ESI-MS: *m/z* 547.3272 $[M+H]^+$ (calcd. for $C_{31}H_{47}O_8$, 547.3265); t_R = 14.4 min.

Fragirubrin G **6**: yellow oil; $[\alpha]_D$ = −2 (*c* 0.1, ACN); ^{1}H NMR ($CDCl_3$, 700 MHz): see Table 1; ^{13}C NMR ($CDCl_3$, 175 MHz): see Table 2; IR (ATR): ν_{max} = 2924, 2854, 1737, 1717, 1641, 1233 cm^{-1}, see Figure S42; UV/vis (ACN): λ_{max} (ε) = 218 (4.23), 327 (4.20) nm; ECD (ACN) $\lambda(\Delta\varepsilon)$: 199 (−5.3), 232 (+1.4), 249 (−0.9), 272 (+3.8), 321 (−3.8) nm, see Figure S44; ESI-MS: *m/z* 529.38 $[M+H]^+$, 527.24 $[M-H]^-$; HR-ESI-MS: *m/z* 529.3160 $[M+H]^+$ (calcd. for $C_{31}H_{45}O_7$, 529.3160); t_R = 17.5 min.

Mosher's analyses

For the preparation of the (*S*)-MTPA ester 1 mg of hybridorubrin A **1** was dissolved in 600 µL of pyridine-*d*5, and 10 µL of (*R*)-MTPA chloride was added. The mixture was incubated at 25 °C for 15 min and ^{1}H NMR, ^{1}H/^{1}H COSY, ^{1}H/^{13}C-HSQC, and ^{1}H/^{13}C-HMBC spectra were measured. ^{1}H NMR (700 MHz, pyridine-*d*5): similar to **1**, but δ_H 1.22 (11'-H_2), 1.60 (12'-H_2), 5.29 (13'-H), 1.63 (14'-H_2), 1.37 (15'-H_2), 0.88 (16'-H_3) ppm. The (*R*)-MTPA ester was prepared in the same manner by addition of 10 µL of (*S*)-MTPA chloride: ^{1}H NMR (700 MHz, pyridine-*d*5): similar to **1**, but δ_H 1.67 (12'-H_2), 5.30 (13'-H), 1.57 (14'-H_2), 1.23 (15'-H_2), 0.82 (16'-H_3) ppm. Results are depicted in Figure S38.

Hybridorubrin B (2×0.7 mg, **2**) was converted analogously. (*S*)-MTPA ester of **2**: ^{1}H NMR (700 MHz, pyridine-*d*5): similar to **2**, but δ_H 2.09 (14'-H_2), 1.69 (15'-H_2), 5.23 (16'-H), 1.68 (17'-H_2), 0.91 (18'-H_3) ppm. (*R*)-MTPA ester of **2**: ^{1}H NMR (700 MHz, pyridine-*d*5): similar to **2**, but δ_H 2.24 (14'-H_2), 1.75 (15'-H_2), 5.24 (16'-H), 1.62 (17'-H_2), 0.80 (18'-H_3) ppm. Results are depicted in Figure S39.

Hybridorubrin C (2×0.5 mg, **3**) was converted analogously. (*S*)-MTPA ester of **3**: ^{1}H NMR (700 MHz, pyridine-*d*5): similar to **3**, but δ_H 1.20 (15'-H_2), 1.59/1.47 (16'-H_2), 5.27 (17'-H), 1.30 (18'-H_3) ppm. (*R*)-MTPA ester of **3**: ^{1}H NMR (700 MHz, pyridine-*d*5): similar to **3**, but δ_H 1.33 (15'-H_2), 1.67/1.52 (16'-H), 5.26 (17'-H_2), 1.24 (18'-H_3) ppm. Results are depicted in Figure S40.

Fragirubrin F (2×0.5 mg, **5**) was converted analogously. (*S*)-MTPA ester of **5**: ^{1}H NMR (700 MHz, pyridine-*d*5): similar to **5**, but δ_H 1.21 (12'-H_2), 1.69/1.57 (13'-H_2), 5.18 (14'-H), 1.66 (15'-H_2), 0.92 (16'-H_3) ppm. (*R*)-MTPA ester of **5**: ^{1}H NMR (700 MHz, pyridine-*d*5): similar to **5**, but δ_H 1.36 (12'-H_2), 1.61/1.54 (13'-H_2), 5.19 (14'-H), 1.36 (15'-H_2), 0.81 (16'-H_3) ppm. Results are depicted in Figure S41.

Epoxidation and MS/MS measurements of 3

In order to locate the position of the double bond in the fatty acid moiety of hybridorubrin C **3**, the sample was epoxidized using *meta*-chloroperoxybenzoic acid (mCPBA) followed by MS/MS analysis, as recently published.[14] At first, 10 µg of **3** was incubated with 10 µg of the mCPBA in 10 µL of DCM at room temperature. The reaction was quenched after 10 min with 490 µL of DCM:ACN 1:1. The same procedure was applied to an authentic reference of *cis*-octadecenoic acid (C18:1(9)).

Then, 1 µL of the samples were injected to an UltiMate® 3000 Series uHPLC (Thermo Fisher Scientific) equipped with a C18 Kinetex column (1,7 µM, 150×2.1 mm, Phenomenex, Torrance, CA/USA) and the following gradient of H_2O+0.1% formic acid (A) and ACN+0.1% formic acid (B): 1% B for 2 min, increasing to 100% B in 18 min, keeping 100% B for further 4 min, flowrate 0.3 mL×min^{-1}. This HPLC was connected to a maXis® HD UHR-ESI-QTOF-MS (Bruker) using the following parameters: scan range: *m/z* 50−1500, ion polarity: negative, capillary voltage: 4500 V, nebulizer pressure: 4.0 bar, dry heater: 200 °C, dry gas: 9.0 L×min^{-1}, collision energy: 20.3−50.7 eV. Results are depicted in Figure S45.

GC analysis of 6

To determine the double bond geometry of the palmitoleic acid moiety of fragirubrin G **6**, 0.5 mg of the compound was hydrolysed by incubating it with MeOH:NaOH (15%) 1:1 for 1 h at 100 °C to yield **6**-fatty acid (FA). Then, **6**-FA, as well as references of 9-*cis*- and 9-*trans*-hexadecenoic acid were derivatized to yield FAME (fatty acid methyl esters) by incubating them in MeOH:HCl (37% w/v) 5:1 for 10 min at 80 °C. Afterwards, the three samples were extracted in the organic phase as described previously.[34] The samples were analysed by gas chromatography on an Agilent 6890N GC with FID (flame ionization detector). Separation of the FAME was carried out with a Macherey Nagel Optima 5 column (5% phenyl, 95% dimethylpolysiloxane; 50 m length; 0.32 mm inner diameter; 0.25 µm film thickness). The retention time of **6**-FAME was compared with those of both references to identify its double bond configuration. The result is depicted in Figure S46.

Bioassays

Minimum inhibitory concentrations (MIC) were determined as described previously.[35] A detailed protocol is given in the Supporting Information. Various test organisms of fungal and bacterial origin were tested. Bacteria: *Bacillus subtilis* (DSM10), *Staphylococcus aureus* (DSM346), *Micrococcus luteus* (DSM1790), *Chromobacterium violaceum* (DSM30191), *Escherichia coli* (DSM1116), *Pseudomonas aeruginosa* (PA14); Mycobacteria: *Mycolicibacterium smegmatis* (ATCC700084); Fungi: *Candida albicans* (DSM1665), *Schizosaccharomyces pombe* (DSM70572), *Mucor hiemalis* (DSM2656), *Pichia anomala* (DSM6766), *Rhodotorula glutinis* (DSM10134). Results are depicted in Table S3.

The cytotoxicity assay against mouse fibroblast cell line L929 as well as human cervical cancer cell line KB 3.1 was performed as described before.[36] Results are depicted in Table S3.

The biofilm formation inhibition assay against *Staphylococcus aureus* (DSM1104) was conducted as described before.[37] Results are depicted in Table 3.

Bioinformatic analysis for gene cluster prediction

The genome of the *H. fragiforme* strain MUCL 51264 was sequenced using PacBio, and gene prediction and annotation was carried out as previously described.[10] Candidate gene clusters were manually identified by blastp searches using various protein sequences as templates (UniProtKB/Swiss-Prot: G3XMC4, G3XMC1, G3XMB9) against a created *H. fragiforme* protein database. The searches were performed with the software Geneious 9.1.8 (https://www.geneious.com). Micro-synteny between related biosynthetic gene cluster was mapped and visualized with the Artemis Comparison Tool (ACT)[38] based on the tblastx output of two aligned sequences calculated on the BLAST webserver. The identified gene cluster were uploaded to GenBank under the accession numbers MN736720 (Hfaza2) and MN736721 (Hfaza1).

Acknowledgments

The authors wish to thank Silke Reinecke and Anke Skiba for expert assistance in the lab. We are also grateful for the help of Aileen Gollasch and Klaus-Peter Conrad for recording the HR-ESI-MS spectra, as well as Christel Kakoschke for performing the NMR measurements. Furthermore, Ulrike Beutling is thanked for assistance with MS/MS measurements. We would like to thank Lucile Wendt for providing the stromatal material and the photograph for the TOC graphic. In addition, we would like to thank Hedda Schrey and Tian Cheng for support with the bioassays as well as Lulu Shao for assistance with the isolation procedure. Boyke Bunk and Cathrin Spröer are acknowledged for PacBio sequencing and Daniel Wibberg for genome annotation. Sebastian Riesinger, Kimberly Borkiet and Natascha Stomberg are thanked for their work in their practical laboratory courses. K. Becker, E. Kuhnert, R. J. Cox and M. Stadler are grateful for a grant from the Deutsche Forschungsgemeinschaft (DFG CO 1328/4-1) in the Priority Programme "Taxon-Omics: New Approaches for Discovering and Naming Biodiversity" (SPP 1991).

The authors declare no conflict of interest.

Keywords: biofilm inhibition • Hypoxylaceae • natural products • pigments • polyketides • structure elucidation • Xylariales •

[1] a) L. Wendt, E. B. Sir, E. Kuhnert, S. Heitkämper, C. Lambert, A. I. Hladki, A. I. Romero, J. J. Luangsa-ard, P. Srikitikulchai, D. Peršoh and M. Stadler, *Mycol. Prog.* **2017**, *17*, 115-154; b) F. Surup, A. Narmani, L. Wendt, S. Pfütze, R. Kretz, K. Becker, C. Menbrivès, A. Giosa, M. Elliott, C. Petit, M. Rohde and M. Stadler, *Fungal Divers.* **2018**, *92*, 345-356.

[2] S. E. Helaly, B. Thongbai and M. Stadler, *Nat. Prod. Rep.* **2018**, *35*, 992-1014.

[3] W. Steglich, M. Klaar and W. Furtner, *Phytochemistry* **1974**, *13*, 2874-2875.

[4] M. Stadler, D. N. Quang, A. Tomita, T. Hashimoto and Y. Asakawa, *Mycol. Res.* **2006**, *110*, 811-820.

[5] J. R. Anderson, R. L. Edwards and A. J. S. Whalley, *J. Chem. Soc., Perkin Trans. 1* **1983**.

[6] R. L. Edwards, V. Fawcett, D. J. Maitland, R. Nettleton, L. Shields and A. J. S. Whalley, *J. Chem. Soc., Chem. Commun.* **1991**.

[7] a) R. Kretz, L. Wendt, S. Wongkanoun, J. J. Luangsa-Ard, F. Surup, S. E. Helaly, S. R. Noumeur, M. Stadler and T. E. B. Stradal, *Biomolecules* **2019**, *9*; b) J. Ondeyka, O. D. Hensens, D. Zink, R. Ball, R. B. Lingham, G. Bills, A. Dombrowski and M. Goetz, *J. Antibiot.* **1992**, *45*, 679-685.

[8] K. T. Yuyama, C. Chepkirui, L. Wendt, D. Fortkamp, M. Stadler and W. R. Abraham, *Microorganisms* **2017**, *5*.

[9] D. Wibberg, M. Stadler, C. Lambert, B. Bunk, C. Spröer, C. Rückert, J. Kalinowski, R. J. Cox and E. Kuhnert, *Fungal Divers.* **2020**.

[10] C. Wang, K. Becker, S. Pfütze, E. Kuhnert, M. Stadler, R. J. Cox and E. Skellam, *Org. Lett.* **2019**, *21*, 8756-8760.

[11] T. R. Hoye, C. S. Jeffrey and F. Shao, *Nat. Protoc.* **2007**, *2*, 2451-2458.

[12] E. Kuhnert, F. Surup, E. B. Sir, C. Lambert, K. D. Hyde, A. I. Hladki, A. I. Romero and M. Stadler, *Fungal Divers.* **2015**, *71*, 165-184.

[13] E. Alexandri, R. Ahmed, H. Siddiqui, M. I. Choudhary, C. G. Tsiafoulis and I. P. Gerothanassis, *Molecules* **2017**, *22*.

[14] Y. Feng, B. Chen, Q. Yu and L. Li, *Anal. Chem.* **2019**, *91*, 1791-1795.

[15] F. D. Gunstone, M. R. Pollard, C. M. Scrimgeour and H. S. Vedanayagam, *Chem. Phys. Lipids* **1977**, *18*, 115-129.

[16] G. Buechi, J. D. White and G. N. Wogan, *J. Am. Chem. Soc.* **1965**, *87*, 3484-3489.
[17] S. Suzuki, T. Hosoe, K. Nozawa, T. Yaguchi, S. Udagawa and K. Kawai, *J. Nat. Prod.* **1999**, *62*, 1328-1329.
[18] R. C. Clark, S. Y. Lee and D. L. Boger, *J. Am. Chem. Soc.* **2008**, *130*, 12355-12369.
[19] C. Chepkirui, K. T. Yuyama, L. A. Wanga, C. Decock, J. C. Matasyoh, W. R. Abraham and M. Stadler, *J. Nat. Prod.* **2018**, *81*, 778-784.
[20] a) A. al Fahad, A. Abood, T. J. Simpson and R. J. Cox, *Angew. Chem. Int. Ed. Engl.* **2014**, *53*, 7519-7523; b) W. Chen, R. Chen, Q. Liu, Y. He, K. He, X. Ding, L. Kang, X. Guo, N. Xie, Y. Zhou, Y. Lu, R. J. Cox, I. Molnar, M. Li, Y. Shao and F. Chen, *Chem. Sci.* **2017**, *8*, 4917-4925; c) Y. He and R. J. Cox, *Chem. Sci.* **2016**, *7*, 2119-2127.
[21] A. O. Zabala, W. Xu, Y. H. Chooi and Y. Tang, *Chem. Biol.* **2012**, *19*, 1049-1059.
[22] P. C. Woo, C. W. Lam, E. W. Tam, C. K. Leung, S. S. Wong, S. K. Lau and K. Y. Yuen, *PLoS Negl. Trop. Dis.* **2012**, *6*, e1871.
[23] a) A. Abood, A. Al-Fahad, A. Scott, A. E.-D. M. S. Hosny, A. M. Hashem, A. M. A. Fattah, P. R. Race, T. J. Simpson and R. J. Cox, *RSC Adv.* **2015**, *5*, 49987-49995; b) A. R. Benitez, S. Tweedy, S. A. Baker Dockrey, A. L. Lukowski, T. Wymore, D. Khare, C. L. Brooks, 3rd, B. A. Palfey, J. L. Smith and A. R. H. Narayan, *ACS Catal.* **2019**, *9*, 3633-3640.
[24] B. Bonsch, V. Belt, C. Bartel, N. Duensing, M. Koziol, C. M. Lazarus, A. M. Bailey, T. J. Simpson and R. J. Cox, *Chem. Commun. (Camb.)* **2016**, *52*, 6777-6780.
[25] note: no stereochemistry was reported for the respective compounds, thus it might differ from **8** and **10** reported herein.
[26] X. Xie, K. Watanabe, W. A. Wojcicki, C. C. Wang and Y. Tang, *Chem. Biol.* **2006**, *13*, 1161-1169.
[27] K. M. Fisch, E. Skellam, D. Ivison, R. J. Cox, A. M. Bailey, C. M. Lazarus and T. J. Simpson, *Chem. Commun. (Camb.)* **2010**, *46*, 5331-5333.
[28] D. N. Quang, T. Hashimoto, M. Stadler and Y. Asakawa, *Tetrahedron* **2005**, *61*, 8451-8455.
[29] Y. Tabata, S. Ikegami, T. Yaguchi, T. Sasaki, S. Hoshiko, S. Sakuma, K. Shin-Ya and H. Seto, *J. Antibiot.* **1999**, *52*, 412-414.
[30] H. Ming Ge, W. Yun Zhang, G. Ding, P. Saparpakorn, Y. Chun Song, S. Hannongbua and R. X. Tan, *Chem. Commun. (Camb.)* **2008**, 5978-5980.
[31] X. Huang, W. Zhang, S. Tang, S. Wei and X. Lu, *Angew. Chem. Int. Ed. Engl.* **2020**, *59*, 4349-4353.
[32] V. Hantke, C. Wang, E. J. Skellam and R. J. Cox, *RSC Adv.* **2019**, *9*, 35797-35802.
[33] a) E. Kuhnert, F. Surup, V. Wiebach, S. Bernecker and M. Stadler, *Phytochemistry* **2015**, *117*, 116-122; b) D. N. Quang, T. Hashimoto, M. Stadler and Y. Asakawa, *J. Nat. Prod.* **2004**, *67*, 1152-1155.
[34] W.-R. Abraham and C. Hesse, *FEMS Microbiol. Ecol.* **2003**, *46*, 121-128.
[35] F. Surup, S. Halecker, M. Nimtz, S. Rodrigo, B. Schulz, M. Steinert and M. Stadler, *Steroids* **2018**, *135*, 92-97.
[36] K. Becker, A.-C. Wessel, J. J. Luangsa-Ard and M. Stadler, *Biomolecules* **2020**, *10*.
[37] K. T. Yuyama, L. Wendt, F. Surup, R. Kretz, C. Chepkirui, K. Wittstein, C. Boonlarppradab, S. Wongkanoun, J. J. Luangsa-ard, M. Stadler and W. R. Abraham, *Biomolecules* **2018**, *8*.
[38] T. J. Carver, K. M. Rutherford, M. Berriman, M. A. Rajandream, B. G. Barrell and J. Parkhill, *Bioinformatics* **2005**, *21*, 3422-3423.

10.1002/chem.202003215

WILEY-VCH

Entry for the Table of Contents

FULL PAPER

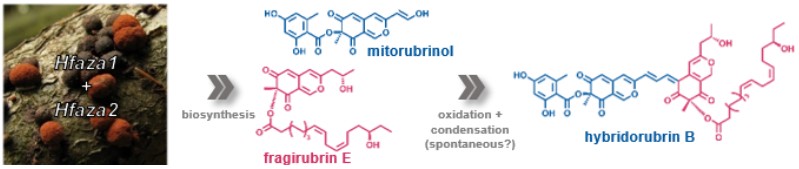

Kevin Becker, Sebastian Pfütze, Eric Kuhnert, Russell J. Cox, Marc Stadler, Frank Surup**

Page No. – Page No.

Hybridorubrins A−D, novel azaphilone dimers from stromata of Hypoxylon fragiforme and insights into the biosynthetic machinery for azaphilone diversification.

Two become one! Hybridorubrins A−D, novel bisazaphilones isolated from the stromata of the ascomycete *Hypoxylon fragiforme*, are composed of mitorubrin- and fragirubrin-type moieties. As revealed by genome analysis, two distantly located biosynthetic gene clusters work together to form these precursors. In contrast to its building blocks, the hybridorubrins exhibit strong inhibitory activity against the biofilm formation of *Staphylococcus aureus*.